The effect of specimen thickness on the shock propagation along the in-fibre direction of an aerospace-grade CFRP laminate

P J Hazell*, C Stennett, G Cooper

Cranfield University, DCMT, Shrivenham, Swindon, SN6 8LA

ABSTRACT

In-fibre measurements of the Hugoniot have been carried out on a carbon-fibre-reinforced-polymer composite. For this material, we have shown at high shock stresses, a two component wave was formed consisting of a fast moving ramped portion and a slower moving shock wave. Changing the thickness of test specimen for a given shock stress resulted in a change in the magnitude and duration of the ramped portion of the wave front. As the shock stress imparted to the target was reduced, or the thickness of the target was increased, the steep shock wave in the rear surface gauge was no longer apparent. Instead a relatively slow rising wave was measured. Consequently, to establish a Hugoniot at lower shock stress levels, relatively thin specimens of target material are required.

Keywords: A. Carbon fibre, **B.** Impact behaviour, Shock response.

*Email: p.j.hazell@cranfield.ac.uk

Tel: +44 (0) 1793 784195

INTRODUCTION

Unlike metals, ceramics and polymers, there is a paucity of data on the dynamic behaviour of carbon fibre composite materials. Most of the work to date has concentrated on relatively low velocity impact studies [e.g 1-6], sphere penetration studies [e.g. 7-14], dynamic tensile and compression tests using servo-hydraulic machines [15-17] and split-hopkinson pressure bar studies [18-23]. Relatively few studies have been done examining the shock behaviour of carbon fibre-based composites and in particular, how the shock wave propagates along the fibre direction.

Understanding how shock waves propagate in these materials is key to our understanding of how these materials respond to high velocity impacts such as those from fragmenting munitions. In particular, there is a requirement to know how the shock propagates in different directions in these anisotropic materials. Understanding the shock propagation along the in-fibre direction is of particular importance for when the material is subjected to highly oblique impacts. At sufficiently high impact velocities, such a loading condition would result in a shock wave that propagated in a direction parallel to one of the fibres.

Attention has been given to examining the shock in the through-thickness direction where the direction of all of the fibres is perpendicular to the loading axis. Dandekar et al. [24] have conducted plate impact experiments on an S2-based GFRP material in the through-thickness direction and shown that the compression curve, as measured in pressure – particle velocity space, of the GRFP lay in-between that of the material's constituent parts. Their results also indicated that there was a linear relationship between shock velocity (U_s) and particle velocity (u_p) of the form

$$U_s = c_0 + Su_p \qquad\qquad (1)$$

where c_0 and S are the shock parameters. A linear Hugoniot in shock velocity –

particle velocity space occurs for a wide range of materials [25] including the RTM6

resin used in the manufacture of these CFRP laminates [26]. It has also been observed

by other researchers studying the shock propagation in the through-thickness direction

of carbon fibre composites [27] and glass fibre composites [28]. Tsai et al. [29] also

studied the shock behaviour of GFRP laminates. In this work they tested the shock

behaviour of different thicknesses of GFRP in the through-thickness direction. They

used a multibeam VALYN™ VISAR (Velocity Interferometer System for Any

Reflector) laser interferometer to measure the particle velocity at the rear surface of

the targets. They noticed a distinct knee in the velocity time profile during the rise

time of the particle velocity profiles in each of the four experiments. Furthermore, the

slope of the velocity time profiles after this knee decreased with the thickness of the

GFRP target i.e. with the distance of wave propagation. The stress level at which the

slope change occurred decreased with increasing GFRP thickness. It was noted that

this phenomenon was similar to the elastic-precursor decay observed in elastic-

viscoplastic materials and for the case of the GFRP tested was understood to be due to

a result of both material and geometric dispersion of the shock wave.

Some attention has also been given to examining the response in the

in-fibre direction. That is, when one of the fibre directions is orientated parallel to the

loading axis. Eden et al. [31] studied the shock behaviour in a 3D quartz phenolic

composite. In this work, they used a streak camera to visualise the wave propagation

in the specimen. Their results also showed that there was a clear distinction between

the wave moving in the fibres orientated with the shock propagation direction and the wave moving in the matrix suggesting that the fibres were acting as wave guides. Holmes and Tsou [32] investigated the shock response of a composite consisting of unidirectional aluminium fibres cast in an epoxy matrix. Again, the fibres were orientated parallel to the loading axis. They showed that the measured shock velocities were constant over a range of thicknesses indicating that the shock itself was steady. Using a streak camera, they noticed a slight waviness in the shock front with a periodicity that corresponded to the fibre spacing. Again, this suggested that the fibres themselves were acting as wave guides. Changing the volume fraction of the aluminium fibres from 25 % to 60 % resulted in their data points falling on different Hugoniots as predicted by the analysis of Tsou and Chou [33].

Millett et al. [27] also studied the effect of orientation on a woven CFRP laminate on its shock behaviour. Using very similar materials and experimental techniques to this work, they showed that in the through-thickness orientation, the material behaved as though it was a simple polymer. When one of the fibre directions was orientated parallel to the loading axis, very different behaviour was observed. The stress pulse had a pronounced ramp, before at sufficiently high stresses, a much faster rising shock occurred above it. Millett et al. [28] also showed similar behaviour in a GFRP material. Similar behaviour was also observed by Hereil et al. [30] who studied the shock response of a 3D carbon-carbon composite. They showed that the response could be decomposed into two separate waves. The first wave is transmitted by the longitudinal fibres and the second wave corresponds to the shock travelling in the 'matrix', that is, all other constituents of the composite including fibres that ran perpendicular to the longitudinal fibres.

In this work, we report experiments that have been conducted to examine the shock behaviour of an aerospace-grade woven CFRP laminate so that one of the fibre directions is aligned perpendicular to the planar shock that is generated on impact by a flyer-plate. The objective of this work was two-fold: (a) to evaluate the effect of sample thickness on the shock propagation in a woven laminate and, (b) to measure the Hugoniot along the in-fibre direction. This work is part of a wider study on the dynamic behaviour of CFRP laminates.

EXPERIMENTAL

Materials used

The materials chosen for this study were woven CFRP laminates that were manufactured using the resin transfer method (RTM). The panel was manufactured with Hexcel G0926 Carbon Fabric with a 5 harness satin weave. The resin used was Hexcel RTM 6 cured for 1 hour 40 minutes at 180 °C and at a pressure of 100 psi. The CFRP panel was 6 mm thick and made from 16 plies with the lay-up sequence (0/90, ± 45, ± 45, 0/90, ± 45, ± 45, 0/90, 0/90, ±45, 0/90, ± 45, 0/90, ±45, 0/90, ± 45, 0/90). The density of the CFRP material, measured using a Micrometrics AccuPyc 1330 gas pycnometer, was 1.512 g/cc ± 0.001 g/cc. The mass fraction of the reinforcement was measured using the acid digestion method according to ASTM D 3171-6, Procedure B. [34] and was found to be 69.7±1.0%

Experimental technique

All the experiments were conducted using the 50-mm single-stage light gas gun [35]. Dural (Al 6082-T6) and copper flyer plates were accelerated to velocities of between 643 m/s and 826 m/s and were used to dynamically load prepared CFRP test specimens.

Ten carbon fibre composite panels, each with a cross-section of 60 mm × 6 mm were stacked and glued together using a two-part epoxy adhesive (Hysol® 0151). As the shock impedances for common epoxy resins are similar to that of the RTM6 resin used in the manufacture of the laminate [26], it was deemed that the addition of the Hysol would not affect the end result. Indeed, this approach was successfully used by Millett et al. [27, 28]. From this block, 1.5, 3.0 and 6.0 mm thick target samples were cut and lapped to ±5μm. The micrograph in Figure 1 shows a portion of the surface of a prepared target specimen, and the two directions of fibres are clearly visible. Note that in this micrograph, the loading axis is in the direction through the page.

Two types of experiments were conducted. Firstly, targets of thicknesses 1.5 mm, 3.0 mm, 6.0 mm and 9.0 mm were each impacted such that a similar shock stress occurred in each of the target specimens. Apart from the 9.0 mm specimen, the test specimens were instrumented with a single manganin pressure gauge (LM-SS-125CH-048), encapsulated between two PMMA layers. This gauge was located on the opposite face to that impacted, and thus recorded the stress history after the shock had passed through the test specimen (see Figure 2(a)); the 9.0 mm specimen also included a front surface gauge. The PMMA was necessary, as noted by Millett et al.,

6

to protect the gauge from premature failure. Calibration of the gauges was to Rosenberg et al. [36].

In the second set of experiments, the test specimens of thickness 3.0 mm, 6.0 mm and 9.0 mm were loaded to different stress levels by varying the velocity and material of the flyer, as noted above. In these experiments, two encapsulated manganin gauges were fixed to both faces of the target specimen so that the shock velocity could be recorded. The first gauge was fixed at the interface between a cover plate (of the same material as the flyer) and the test specimen. This gauge was encapsulated between two layers of Mylar 50 µm thick, to provide electrical insulation and to give mechanical protection. The second gauge, located at the rear of the target, was fixed between a layer of PMMA c. 1.5 mm thick, and a PMMA block of c. 12 mm thick, so that the thinner PMMA layer was in contact with the test specimen. A typical target set-up is given schematically in Figure 2(b).

Before firing, the thickness of each test specimen was carefully measured, so that the distance between the gauges was accurately known. By measuring the time of arrival of the shock at each gauge, the (assumed constant) shock velocity (U_s) could be calculated from the transit time (Δt) of the shock across the specimen taking into account the offset distance of the rear embedded gauge from the rear of the target specimen and the shock behaviour of PMMA [37]. Hugoniot data for our flyer-plate materials were taken from Marsh [38] and the velocities of the projectile were measured by using a sequential pin shorting system to an accuracy of 0.5%. Fast digital storage oscilloscopes (2 GS/s) were used to capture the arrival and shape of the shock; subsequent data reduction and analysis was done on a PC. The impedance matching technique [39] was used to derive the particle velocity behind the shock given the measurements noted above.
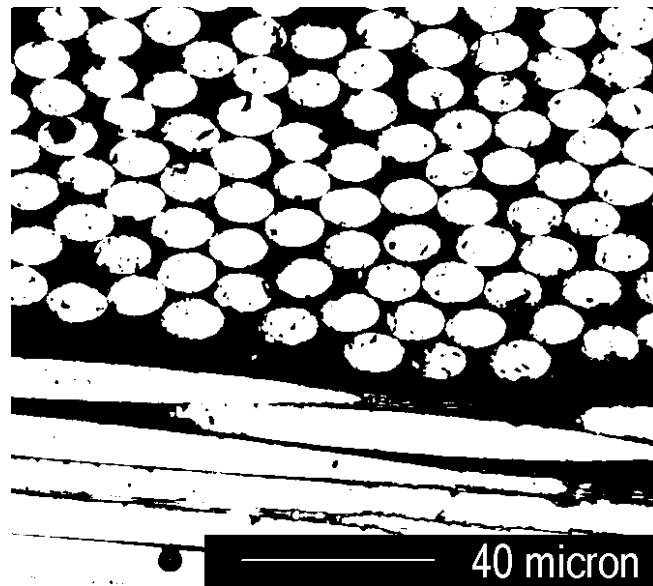
Figure 1: Micrograph showing 0° and 90° fibres, the black area indicates the presence of the RTM6 resin.
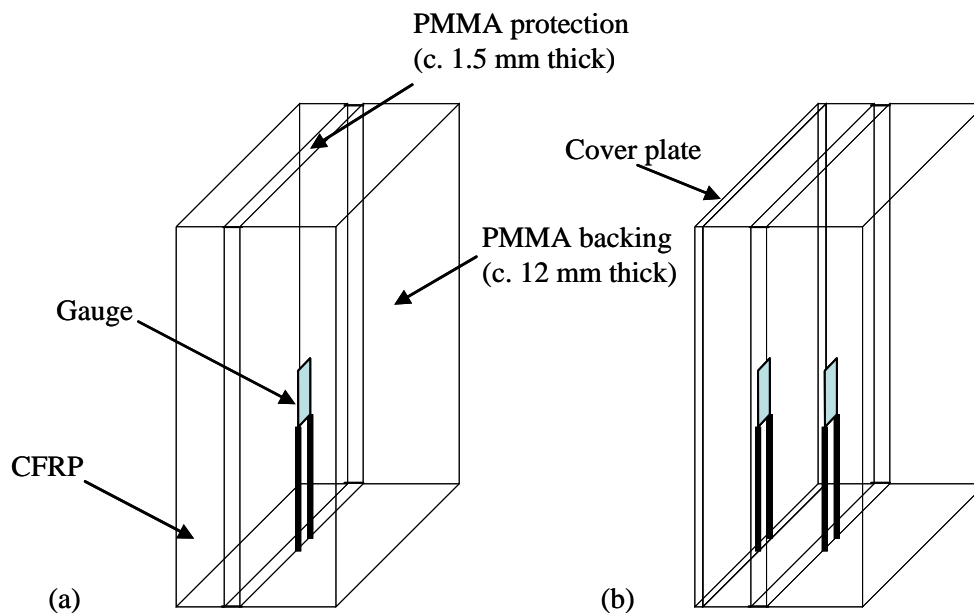

Figure 2: Two types of target configuration used in these experimental trials.

RESULTS AND DISCUSSION

As noted by Millett et al. [27], unlike isotropic single-phased materials, the shock structure as recorded by the manganin gauges along the fibre direction is

complex. Figure 3 shows the stress histories recorded by the two manganin gauges in an experiment where a 5-mm thick copper plate impacted the target at a velocity of 811m/s. The front-surface gauge was encapsulated in a 50 µm Mylar package and the rear gauge was protected from the composite by 1.62 mm of PMMA. It can be seen that initially, the front gauge senses the shock propagating through the target assembly and eventually fails (1) probably due to the gauge being punctured by the longitudinal carbon fibres.
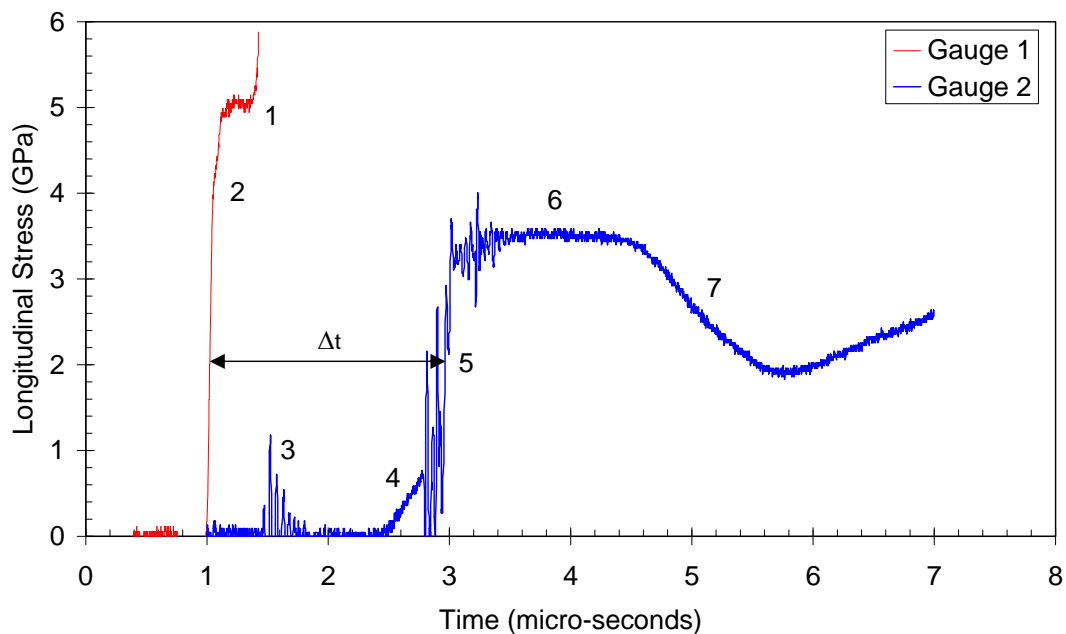

Figure 3: In-fibre shock trace; the annotations (1-7) are referred to in the text. This result is for a 5-mm thick Cu flyer impacting a 6-mm thick CFRP in-fibre target at 811 m/s.

The reason for the change in slope (2) towards the top end of the initial shock is unclear. Other traces showed a break in slope around this region and may suggest failure of the adhesive layer between the gauge package and the CFRP. The spurious noise at (3) is due to the front gauge failing and the inevitable subsequent cross-talk between the gauges. Consequently, the second gauge continues to pick up interference for the duration of the experiment. At (4) the rear face gauge observes a relatively

9

gentle slope to approximately 1.1 GPa. This has been observed by other researchers examining the shock response of a 3D carbon-fibre composite material [30]. Here the low amplitude ramp was interpreted as being a high velocity wave transmitted along the fibres orientated parallel to the loading axis. Measurements from an experiment using a 3-mm thick sample, indicate a propagation velocity of 6.2 mm/µs for the onset of the ramped portion. Previous analysis by Millett et al. [27] has concluded that the arrival time of the onset of this low amplitude ramp corresponds to a transit velocity of ca. 7 mm/µs regardless of shock stress, although they noted that his data showed considerable scatter. They suggested that if this wave had been transmitted down the fibres, it would be largely elastic in nature. At a stress of approximately 1.1 GPa, there is a sharp rise to maximum stress (5), which is attributed to the arrival of the 'main shock' that is transmitted through the 'matrix' composed of the binder and the fibres not aligned parallel to the loading axis. Finally, the maximum stress is reached in the PMMA encapsulation before the arrival of the release wave (7).

The stress history shown in Figure 3 is typical of the experiments in which the impact velocity and flyer material were chosen to form a stress of 5-6 GPa in the target, and where the target specimens were of 6 mm or greater thickness. However, in those experiments where the impact stress was lower, the structure of the stress history on the back surface gauges did not resemble that of a fast rising shock as seen in Figure 3. Furthermore, due to the presence of the cross-talk from the front gauge there was considerable uncertainty in the interpretation of the physical processes.

The effect of sample thickness on the shock behaviour

To investigate the physical processes further, we conducted a series of three well-resolved experiments using the test specimen set-up shown in Figure 2(a) where there was no front gauge. In these experiments, 5-mm thick copper flyers impacted the target specimens a fixed velocity of c. 700 m/s. The thicknesses of the specimens tested were : 1.52 mm, 3.00 mm, 6.05 mm. These data were compared to data from a previous experiment on a 9.06 mm thick specimen that used the set-up shown in Figure 2(b). With this thicker specimen an aluminium flyer impacted the target at 824 m/s to produce a shock stress in the target that was similar to the thinner targets tested. This particular experiment also included a front surface gauge in an attempt to evaluate the wave velocity. However due to the presence of the front gauge, that failed at an early stage of the experiment, some spurious noise was produced. Consequently an FFT was applied to the data to remove the offending high frequency components (50- 570 MHz). All other traces presented required no such filtering. A single manganin gauge encapsulated by the PMMA layers was placed on the rear face of the target to record the stress history after its passage through the test specimen. The stress histories for all four experiments are shown together in Figure 4. Note that the time axis has been adjusted so that all four traces are coincident, and that the stresses are recorded in the PMMA protection at the rear of the specimen, rather than directly in the target material.
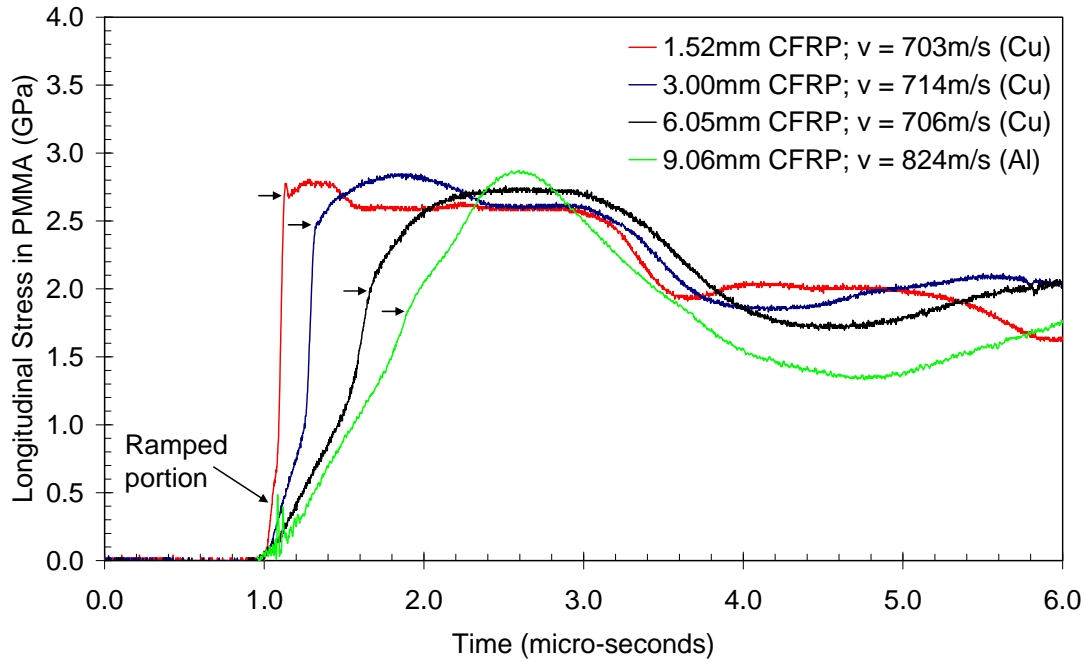
Figure 4: The effect of sample thickness on the structure of the shock wave as recorded by a single embedded manganin gauge located on the rear face of the target; the velocities of impact and the flyer materials used are labelled.

It can be seen that, as the target thickness increases, the ramped portion of the stress history becomes more pronounced. The durations of the ramped portion are 0.08 µs, 0.26 µs, 0.53 µs and 0.81 µs for target thicknesses of 1.52 mm, 3.00 mm, 6.05 mm and 9.06 mm respectively. The magnitude of the ramped portion (measured from the onset of the ramp until the change to a steeper slope) also increased with target thickness, with magnitudes of 0.69 GPa, 1.00 GPa, 1.15 GPa and 1.50 GPa for the four experiments conducted. Note however, that Millett et al. [27] showed that for an impact of 936 m/s by a copper flyer on a 10 mm thick sample, the ramped portion terminated at a stress of 1.09 GPa at a time of 785 ns after onset, for an impact stress of 5.75 GPa – a higher impact stress than recorded in Figure 4. This suggests that the magnitude and duration of the ramped phase of the stress recorded at the rear surface of the target specimen was dependent upon both the target thickness and the impact

12

stress. This part of the wave form has previously been attributed to be the fast moving largely elastic portion in the fibres. However the increasing length and magnitude and shape of this part of the wave demands explanation. One possibility is that energy is continuously being lost from the fibres into the surrounding matrix material. Consequently this ramped portion is initially a sharp elastic rise that is smeared with distance. Indeed, this is consistent with the decrease in the gradient that is seen with the 1.5 mm, 3.0 mm and 6.0 mm sample and to a lesser extent, with the 9.0 mm sample. However, we should point out that a certain amount of caution should be applied in interpreting this result (for the 9.0 mm sample) due to the filtering that was applied. On the other hand, the nature of ramped portion may be attributed to the complexity of the laminate design used in this experimental programme. Fibre waviness and the presence of the +/- 45° fibres will both result in a variable arrival of the wave at the manganin gauge leading to a gradual increase in resistance (and therefore stress) in the gauge material. However it is difficult to reconcile this latter explanation with the observed magnitude and duration of the ramped portion.

The relatively sharp rise after the ramped portion of the stress histories (attributed to the arrival of the wave propagating through the 'matrix') is observed to terminate at a decreasing stress as the target thickness increases. This stress is indicated by the arrows in Figure 4. Beyond this point, the stress continues to rise at a slower rate up to a maximum of 2.8 GPa. This implies that as the shock is travelling through the thickness of the material, it is being dispersed. Note too, the reduction in the gradient as the thickness of the material is increased. Tsai et al. [29] studied the structure of shock waves in S2-based polymer reinforced composites of varying thicknesses. They noted that as the thickness of the material was increased, there was a noticeable slope change in the profile of the pulse. The stress level at which the

slope change occurred decreased with increasing GFRP thickness and was thought to be due to the dispersive nature of these materials. Although Tsai et al. was not examining the in-fibre behaviour, their work correlates with these results. It is interesting to note that the dispersion of the shock occurs for a 6 mm thick sample at c. 700 m/s (with a Cu flyer) but not at higher velocities of impact for the same thickness. This result suggests that the dispersion of the shock is dependent on the thickness of the target as well as the strength of the shock with weaker shocks being more susceptible to dispersion.

There are two possibilities behind this dispersion. Firstly, energy is being deposited into the matrix before the shock arrives.   Due to the relatively low impedance of the surrounding resin, and the low transverse dimension in the rods, the state of strain in the carbon fibres will cease to be 1D at a short distance from the impact surface. As previously discussed the waves propagate along the fibres, energy is lost to the surrounding matrix prior to the arrival of the shock in that material leading to the wave dispersion observed in Figure 4. Another possible explanation is that, wavelets emerging from the carbon fibres result in a state of complex ringing between fibre bundles in the matrix leading to a state that is unable to sustain a shock wave in the material. That is, unless the shock is of sufficient magnitude (as occurred with the high velocity shots) or the ringing is relatively small (as occurred for our thin targets). Changing the fibre spacing would, if this was the case, affect the behaviour of shock propagation.

Finally, we note that the thinner thicknesses tested reach a Hugoniot stress of 2.6 GPa in the PMMA whereas the 6.05-mm thick sample is subjected to a higher stress. Although the reason for the higher stress is not clear, it maybe due to the dispersive nature of the wave leading to a longer duration initial 'hump'.

Consequently, the Hugoniot stress is not achieved due to the arrival of the release wave from the rear of the 5-mm thick Cu flyer. Note too that the 3.00-mm thick sample Hugoniot stress is slightly higher than the 1.52-mm thick sample stress. This is consistent with the slightly higher impact velocity in this case.

The in-fibre Hugoniot

As we have shown, it is possible to observe a reasonably well-defined shock in the back surface gauge if the separation between the two gauges is reduced. Using this technique, it was possible to establish a Hugoniot along the in-fibre direction. This is shown below in Figure 5: the error bars indicate the uncertainty in our measurement of the shock arrival times at each gauge (and hence the measured shock velocity) due the presence of spurious noise occasionally picked up by the rear gauge as the front gauge failed. For most materials a linear fit can be used to describe the shock particle velocity relationship over a limited particle-velocity range according Equation 1. Indeed, Millett et al. found that the Hugoniot for the CFRP laminate in the through-thickness direction could be described by Equation 1 and showed that the parameters of c_0 and S were 3.23 mm/µs and 0.92 respectively. The Hugoniot is shown in Figure 5 and includes three data points where a fast rising shock wave was measured in the rear gauge by Millett et al. The measured values of S and c_o were 2.27 and 2.26 mm/µs respectively over the limited particle-velocity range of interest, and for shocks along the fibre direction. This Hugoniot is similar to the RTM6 resin used to manufacture these CFRP laminates where the measured values of S and c_o were 1.55 and 2.65 mm/µs respectively [26]. However, the resin has a bulk density of 1.14 g/cc as opposed to 1.51 g/cc measured for this CFRP resulting in a different

shock impedance. Data points for the resin, over the particle velocity range of interest are also included in Figure 5 for completeness.
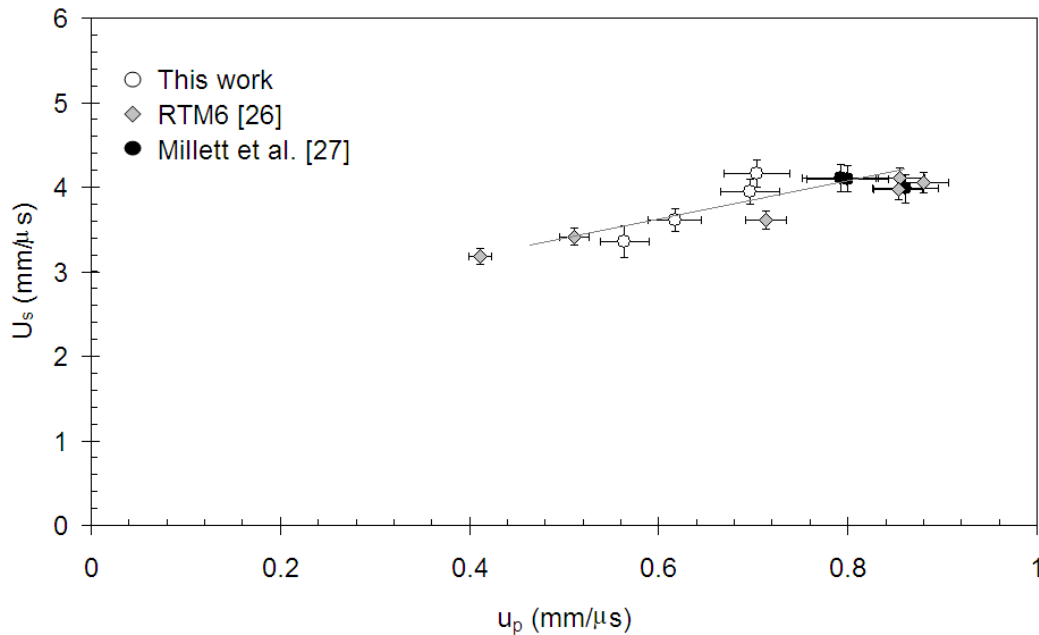

Figure 5: The CFRP in-fibre Hugoniot. Data from Millet et al [27] is included as well as data points from the measured Hugoniot of the RTM6 resin [26].

CONCLUSIONS

A series of plate impact experiments have been conducted on a CFRP laminate where the plane of impact was perpendicular to one of the fibre directions. These results showed that at high shock stresses, a two component wave was formed consisting of a fast moving ramped portion and a slower moving shock wave. Changing the thickness of test specimen for a given shock stress resulted in a change in the magnitude and duration of the ramped portion of the wave front. As the shock stress imparted to the target was reduced, or the thickness of the target was increased, the steep shock wave in the rear surface gauge was no longer apparent. Instead a relatively slow rising wave was measured. However, reducing the spatial separation

between the front surface and backs surface gauges resulted in the shock being measured. We were able to observe shock propagation in c. 3.0 mm thick samples that were subjected to a shock stress as low as c. 3.4 GPa. Consequently, using data from Millett et al. [27] we were able to establish the in-fibre Hugoniot for this material over a limited particle-velocity range and it was given by $U_s=2.27+2.26u_p$ ($\rho_0 = 1.512$ g/cc).

ACKNOWLEDGEMENT

REFERENCES

1. Cantwell WJ, Morton J. The impact resistance of composite materials — a review. Compos 1991;22(5):347-362.

2. Richardson MOW, Wisheart MJ. Review of low-velocity impact properties of composite materials. Compos Part A: Appl Sci and Manuf 1996;27(12):1123-1131.

3. Morton J, Godwin EW. Impact response of tough carbon fibre composites. Composite Structures 1989;13:1-19.

4. Cantwell WJ, Curtis PT, Morton J. An assessment of the impact performance of CFRP reinforced with high-strain carbon fibres. Compos Sci and Tech 1986; 25(2):133-148.

5. Curtis PT, Bishop SM. An assessment of the potential of woven carbon fibre-reinforced plastics for high performance applications. Compos 1984;15(4):259-265.

6. Robinson P, Davies GAO, Impactor mass and specimen geometry effects in low velocity impact of laminated composites. Int J of Impact Engng 1992;12(2):189-207.

7. Bland PW and Dear JP, Observations on the impact behaviour of carbon–fibre reinforced polymers for the qualitative validation of models, Compos Part A Appl Sci Manuf 2001;32:1217–1227.

8. Hammond RI, Proud, WG, Goldrein HT and Field, JE. High-resolution optical study of the impact of carbon-fibre reinforced polymers with different lay-ups. Int J Impact Engng 2004;30:69-86.

9. Tanabe Y, Aoki M. Stress and strain measurements in carbon-related materials impacted by high-velocity steel spheres. Int J Impact Engng 2003;28:1045-1059.

10. Cantwell WJ and Morton J. Impact perforation of carbon fibre reinforced plastics. Compos Sci and Tech 1990;38:119-141.

11. Hosur MV, Vaidya UK, Ulven C and Jeelani S, Performance of stitched/unstitched woven carbon/epoxy composites under high velocity impact loading, Compos Struct 2004;64:455–466.

12. Lopez-Puente J, Zaera R and Navarro C, Experimental and numerical analysis of normal and oblique ballistic impacts on thin carbon/epoxy woven laminates, Compos Part A: Appl Sci and Manuf 2008;39:374-387.

13. Hazell PJ, Kister G, Bourque P, Cooper G. Normal and oblique penetration of woven CFRP laminates by a high velocity steel sphere. Compos Part A: Appl Sci and Manuf 2008; 39:866-874.

14. Hazell PJ, Kister G, Cooper G. Impact and penetration of a two-part bonded CFRP composite panel by a high velocity steel sphere. Submitted to Compos Part A: Appl Sci and Manuf.

15. Hsiao HM, Daniel IM. Strain rate behavior of composite materials. Compos Part B: Engng 1998; 29:521-533.

16. Gilat A, Goldberg RK, Roberts GD, Experimental study of strain-rate-dependent behavior of carbon/epoxy composite. Compos Sci and Tech 2002; 62: 1469-1476.

17. Fitoussi J, Meraghni F, Jendli Z, Hug G, Baptiste D. Experimental methodology for high strain-rates tensile behaviour analysis of polymer matrix composites. Compos Sci and Tech 2005; 65: 2174-2188.

18. Sierakowski RL. Strain rate effects in composites. Appl Mech Rev 1997;50: 741-761.

19. Griffiths LJ, Martin DJ, A study of the dynamic behaviour of a carbon fibre composite using the split Hopkinson pressure bar. J Phys D: Appl Phys 1974; 7: 2329-2341.

20. Hosur MV, Adya M, Vaidya UK, Mayer A, Jeelani S. Effect of stitching and weave architecture on the high strain rate compression response of affordable woven carbon, epoxy composites. Compos Struc 2003;59:507 – 523.

21. Bing Q, Sun CT, Modeling and testing strain rate-dependent compressive strength of carbon / epoxy composites. Compos Sci and Tech 2005;65: 2481 – 2491.

22. Rhee KY, Kim HJ, Park SJ. Effect of strain rate on the compressive properties of graphite/epoxy composite in a submarine environment. Compos Part B: Engng 2006; 37: 21-25.

23. Jadhav A, Woldesenbet E, Pang S. High strain rate properties of balanced angle-ply graphite/epoxy composites. Compos Part B: Engng 2003;34: 339-346.

24. Dandekar DP, Hall CA, Chhabildas LC, Reinhart WD. Shock response of a glass-fiber-reinforced polymer composite. Compos Struc 2003;61: 51-59.

25. Ruoff L. Linear Shock-Velocity-Particle-Velocity Relationship, J of Appl Phys 1967;38:4976 -.

26. Hazell PJ, Stennett C, Cooper G. The shock and release behavior of an aerospace-grade cured aromatic amine epoxy resin. Polymer Compos 2008; 29 (10): 1106-1110. DOI 10.1002/pc.20614.

27. Millett JCF, Bourne NK, Meziere YJE, Vignjevic R, Lukyanov A, The effect of orientation on the shock response of a carbon fibre-epoxy composite, Compos Sci and Tech 2007;67:3253-3260

28. Millett JCF, Meziere YJE, Bourne NK. The response to shock loading of a glass-fibre-epoxy composite: Effects of fibre orientation to the loading axis. J Phys D: Appl Phys 2007; 40 (17): 5358-5365

29. Tsai L, Prakesh V, Rajendran AM, Dandekar DP, Structure of shock waves in glass fiber reinforced polymer matrix composites. Appl Phys Lett 2007; 90: 061909.

30. Hereil PL, Allix O, Gratton M. Shock behaviour of 3D carbon-carbon composite. J. Phys. IV 1997; 7: 529-534.

31. Eden G, Carden MH, Collyer AM, Smith CPM. Shock wave propagation in a 3-D quartz phenolic composite. In: Schmidt SC, Johnson JN, Davison LW (editors). Shock compression of condensed matter – 1989, Elsevier (1990).

32. Holmes BS, Tsou FK. Steady shock waves in composite materials J Appl Phys 1972;43: 957–961.

33. Tsou FK, Chou PC. Analytical study of Hugoniot in unidirectional fiber reinforced composites. J Comps Mater 1969;3:500-514.

34. ASTM Standard D 3171-06. Standard Test Methods for Constituent Content of Composite Materials. ASTM International, 2006.

35. Bourne NK. A 50mm bore gas gun for dynamic loading of materials and structures. Meas Sci Technol 2003; 14: 273-278.

36. Rosenberg Z, Yaziv D Partom Y. Calibration of foil-like manganin gauges in planar shock wave experiments. J. Appl. Phys 1980; 51: 3702.

37. Barker LM and Hollenbach RE. Shock-wave studies of PMMA, fused silica and sapphire. J Appl Phys 1970; 41:4208-4226.

38. Marsh SP. LASL Shock Hugoniot Data. University of California Press, Los Angeles, (1980).

39. Davison L and Graham RA. Shock compression of solids. Phys Reports (Review Section of Physics Letters) 1979;55:255-379.